# Nuclear Imaging Techniques for the Assessment of Hepatic Function in Liver Surgery and Transplantation

Wilmar de Graaf[1], Roelof J. Bennink[2], Reeta Veteläinen[1], and Thomas M. van Gulik[1]

*[1]Department of Surgery, Academic Medical Center, Amsterdam, The Netherlands; and [2]Department of Nuclear Medicine, Academic Medical Center, Amsterdam, The Netherlands*

**Learning Objectives:** On successful completion of this activity, participants should be able to describe (1) the relevance of assessment of liver function in liver surgery and transplantation; (2) the technical background of $^{99m}$Tc-GSA scintigraphy and $^{99m}$Tc-mebrofenin hepatobiliary scintigraphy; and (3) the role of $^{99m}$Tc-GSA scintigraphy and $^{99m}$Tc-mebrofenin hepatobiliary scintigraphy for preoperative assessment of future remnant liver function, follow-up after preoperative portal vein embolization, and evaluation of postoperative liver regeneration.

**Financial Disclosure:** The authors of this article have indicated no relevant relationships that could be perceived as a real or apparent conflict of interest.

**CME Credit:** SNM is accredited by the Accreditation Council for Continuing Medical Education (ACCME) to sponsor continuing education for physicians. SNM designates each JNM continuing education article for a maximum of 1.0 AMA PRA Category 1 Credit. Physicians should claim only credit commensurate with the extent of their participation in the activity.

For CE credit, participants can access this activity through the SNM Web site (http://www.snm.org/ce_online) through May 2011.

This review describes the application of 2 nuclear imaging techniques for assessment of hepatic function in the setting of liver surgery and transplantation. The biochemical and technical background, as well as the clinical applications, of $^{99m}$Tc-labeled diethylenetriaminepentaacetic acid galactosyl human serum albumin (GSA) scintigraphy and hepatobiliary scintigraphy (HBS) with $^{99m}$Tc-labeled iminodiacetic acid derivates is discussed. $^{99m}$Tc-mebrofenin is considered the most suitable iminodiacetic acid agent for $^{99m}$Tc-HBS. $^{99m}$Tc-GSA scintigraphy and $^{99m}$Tc-mebrofenin HBS are based on 2 different principles. $^{99m}$Tc-GSA scintigraphy is a receptor-mediated technique whereas HBS represents hepatic uptake and excretion function. Both techniques are noninvasive and provide visual and quantitative information on both total and regional liver function. They can be used for preoperative assessment of future remnant liver function, follow-up after preoperative portal vein embolization, and evaluation of postoperative liver regeneration. In liver transplantation, these methods are used to assess graft function and biliary complications.

**Key Words:** hepatology; SPECT; SPECT/CT; $^{99m}$Tc-GSA scintigraphy; hepatobiliary scintigraphy; liver function; mebrofenin

**J Nucl Med 2010; 51:742–752**
DOI: 10.2967/jnumed.109.069435

Surgical resection is still the most effective treatment for patients with hepatic malignancies. Because of improved surgical techniques and perioperative care, extended resections are performed with greater frequency. Extended resections can, however, result in a small postoperative remnant liver with increased risk of postoperative liver failure, especially in patients whose liver parenchyma is compromised because of steatosis, cholestasis, or fibrosis (*1,2*). Treatment of posthepatectomy liver failure remains difficult, and mortality is substantial. Preoperative evaluation of future remnant liver (FRL) function is therefore important to determine whether a patient can safely undergo an extended liver resection. The availability of preoperative portal vein embolization (PVE) has increased the importance of preoperative assessment of regional hepatic function (*3*). PVE induces atrophy of the embolized, tumor-bearing liver segments with compensatory hypertrophy of the nonembolized lobe, thereby increasing FRL volume and function. PVE reduces the risk of postoperative liver insufficiency in patients with a marginal FRL (*4*). The individual hypertrophic response is variable (*4,5*), indicating the need to quantify the increase in FRL function after PVE.

The unique capacity of the liver to regenerate is important for the clinical outcome of donor and recipient after living donor liver transplantation, as well as for patients undergoing partial liver resection. Liver regeneration is influenced by many factors, including the presence of coexisting parenchymal liver diseases (*6*). Impaired liver regeneration can cause serious clinical problems such as delayed recovery of postoperative liver function and increased risk of postoperative liver failure. It is consequently imperative to evaluate the recovery of liver function after liver surgery.

The liver encompasses multiple functions, including metabolic, synthetic, and detoxifying functions. In recent

Received Aug. 24, 2009; revision accepted Dec. 4, 2009.
For correspondence contact: Thomas M. van Gulik, Department of Surgery, Academic Medical Center, Meibergdreef 9, IWO-1, 1105 AZ Amsterdam, The Netherlands.
E-mail: t.m.vangulik@amc.uva.nl

decades, several liver function tests have been developed, each reflecting a separate component of the broad spectrum of liver function. $^{99m}$Tc-labeled diethylenetriaminepentaacetic acid galactosyl human serum albumin (GSA) scintigraphy and hepatobiliary scintigraphy (HBS) with $^{99m}$Tc-labeled iminodiacetic acid (IDA) derivates are 2 nuclear imaging techniques used for noninvasive evaluation of liver function. This review discusses the biochemical and technical background, as well as the clinical applications, of $^{99m}$Tc-GSA scintigraphy and HBS for the assessment of hepatic function in liver surgery and transplantation.

## THE DEVELOPMENT OF NEW TECHNIQUES FOR ASSESSMENT OF LIVER FUNCTION

The Child–Pugh score is a widely used clinical scoring system that includes biochemical parameters (plasma bilirubin albumin and prothrombin time) together with clinical parameters (presence of encephalopathy and ascites). The Child–Pugh scoring system is conventionally used in selecting patients with hepatocellular carcinoma and cirrhosis for resection or transplantation. It provides merely indirect information on FRL function and can be unreliable for predicting clinical outcome after liver resection, especially in noncirrhotic patients (*7,8*).

Indocyanine green (ICG) clearance and galactose elimination capacity are dynamic quantitative liver function tests. ICG is cleared from plasma by hepatocyte transporters located on the basolateral membrane and subsequently excreted into the bile (*9*). Galactose elimination capacity measures the rate of galactose elimination from the blood—a rate that depends mainly on phosphorylation of galactose by galactokinase (*10*). Although the ICG clearance test (*11,12*) and galactose elimination capacity (*13*) have the ability to preoperatively predict morbidity and mortality after partial hepatectomy, they can be unreliable (*7,14*) because they measure global liver function and not specific FRL function. The ICG clearance test is the most frequently used quantitative liver function test in liver surgery and transplantation (*15*). Other clinically applied liver function tests include the monoethylglycinexylidide test, which measures hepatic metabolism of lidocaine through the cytochrome p450 pathway (*16,17*), the caffeine clearance test, and the aminopyrine breath test (*7*), all of which provide information on total liver function only.

CT volumetry, in which liver volume is used as an indirect measurement of liver function, is currently the established method to determine whether a patient can safely undergo liver resection (*15,18*). Although there are no official guidelines, an FRL volume larger than 25% (15%–40%) of total liver volume is considered sufficient for a safe resection in patients with normal liver parenchyma, whereas in patients with a compromised liver (e.g., fibrosis, steatosis, or cholestasis), more than 40%–50% is preferred (*15,19*). These separate ranges of what is considered sufficient FRL volume necessitate the preoperative assessment of liver parenchyma quality by liver biopsy to identify patients with increased surgical risk. Preoperative liver biopsy is not routinely performed, because of the potentially unequal distribution of parenchymal damage (*20*) and the risk of complications (*21,22*). As a result, the quality of the liver parenchyma remains frequently uncertain, rendering preoperative risk analysis by CT volumetry unreliable.

In recent decades, several nuclear imaging techniques have been developed as noninvasive methods for evaluating liver function. $^{131}$I-rose bengal was one of the first agents used for HBS. $^{131}$I-rose bengal is taken up from the circulation by hepatocytes and excreted into the biliary system. Rose bengal fell in disfavor because of several disadvantages, including its slow hepatic clearance and significant β-radiation, which limits the dose that can safely be administered, thereby resulting in poor imaging characteristics. $^{99m}$Tc proved a more suitable isotope for scintigraphy because of its excellent physical characteristics. Several $^{99m}$Tc-labeled agents have been developed, including $^{99m}$Tc-sulfur colloid, $^{99m}$Tc-GSA, and $^{99m}$Tc-IDA. The latter 2 radiopharmaceuticals can be used for assessment of hepatocyte function, whereas $^{99m}$Tc-sulfur colloid scintigraphy is based on the principle of phagocytosis by the reticuloendothelial cells of the liver, thereby visualizing RE activity.

## $^{99M}$TC-GSA SCINTIGRAPHY

### Background

The asialoglycoprotein receptor is present only in mammalian hepatocytes and is specific for asialoglycoproteins, which are formed after the removal of sialic acid from endogenous glycoproteins by sialidases. The asialoglycoprotein receptor consists of 2 subunits (human hepatic lectins 1 and 2) and is expressed on the hepatocyte sinusoidal surface adjoining the extracellular space of Disse (*23*). Asialoglycoproteins bind to asialoglycoprotein receptors and are subsequently taken up by receptor-mediated endocytosis and delivered to lysosomes for degradation. A significant decrease in asialoglycoprotein receptors together with accumulation of plasma asialoglycoproteins is seen in patients with chronic liver diseases (*24,25*). At first, $^{99m}$Tc-labeled galactosylneoglycoalbumin was developed as a synthetic asialoglycoprotein to visualize and quantify its hepatic binding to the asialoglycoprotein receptor (*26*). For clinical use, $^{99m}$Tc-GSA, which is commercially available in an instant labeling kit in Japan, was developed (*27*). The liver is the only uptake site for $^{99m}$Tc-GSA, which is therefore an ideal agent for functional liver scintigraphy. The parameters obtained from planar $^{99m}$Tc-GSA scintigraphy proved valuable for the assessment of liver function in cirrhotic patients and demonstrated a strong correlation with conventional liver function tests (i.e., antithrombin III, bilirubin, prothrombin time, ICG clearance, Child–Pugh classification, and histology [hepatic activity index score]) (*28,29*). A discrepancy between the ICG clearance test and $^{99m}$Tc-GSA scintigraphy is described in 9%–20% of the patients in whom the

histologic severity of disease is better reflected by $^{99m}$Tc-GSA scintigraphy (*30,31*). $^{99m}$Tc-GSA scintigraphy is also effective in assessing hepatic function in patients with hyperbilirubinemia (*32–34*).

## Kinetics and Quantitative Measurement of Liver Function

After an intravenous bolus of $^{99m}$Tc-GSA, dynamic $^{99m}$Tc-GSA scintigraphy images are obtained by a γ-camera positioned over the heart and liver region. The blood clearance and hepatic uptake are obtained by generating regions of interest (ROIs) of the heart and liver, respectively. For actual kinetics of $^{99m}$Tc-GSA receptor binding, 3 models are commonly applied.

Vera et al. developed a 3-compartment model of a bimolecular chemical reaction (*35*). Required for calculations in this model are time–activity curves of liver and heart; the patient's height, weight, and hematocrit level; and a portion of the injected dose from a blood sample. Five independent parameters are calculated: receptor concentration, receptor affinity (forward binding rate), hepatic plasma volume, extrahepatic plasma volume, and hepatic plasma flow. The receptor concentration is the most accurate index for hepatic function (*36,37*).

A 5-compartment model based on a Michaelis–Menten type of kinetics for receptor–ligand binding was introduced as a noninvasive approach, requiring no blood samples (*38*). Blood flow and maximal removal rate ($R_{max}$) of $^{99m}$Tc-GSA (mg/min) from plasma are calculated from time–activity curves of heart, liver, and lung (background). Miki et al. introduced a 7-compartment model that included receptor-mediated endocytosis and receptor recycling (*39*). The model permits quantitative measurement of total receptor amount ($R_{tot}$) and hepatic blood flow, without blood samples. $R_{tot}$ correlates with the number of viable hepatocytes and can be used to assess functional liver mass (*40*).

Although many different parameters can be calculated from the different kinetic models, they are highly complex and therefore not widely used in the context of liver surgery. Tables 1 and 2 provide an overview of frequently used parameters in this field. Hepatic uptake ratio and blood clearance ratio of $^{99m}$Tc-GSA are the most commonly used parameters determined from planar dynamic $^{99m}$Tc-GSA scintigraphy (Fig. 1). Blood clearance ratio is calculated by dividing the radioactivity of the heart ROI at 15 min after $^{99m}$Tc-GSA injection by that at 3 min after injection (HH15). Hepatic uptake ratio is calculated by dividing the radioactivity of the liver ROI by the radioactivity of the liver-plus-heart ROIs at 15 min after injection (LHL15) (*27,29,41*). The modified receptor index is determined by dividing LHL15 by HH15 (*29*).

Static $^{99m}$Tc-GSA SPECT has been introduced to improve the assessment of segmental liver function and to measure functional liver volume (*33,42–44*). The outline extraction method is a simple technique to calculate functional liver volume using a specific cutoff value to automatically outline the liver (*33*). However, it does not incorporate regional functional differences within the included volume. Therefore, Satoh et al. described a more precise method for calculating functional liver volume depending on the degree of $^{99m}$Tc-GSA radioactivity in each voxel (*43*). First, the voxel with maximal counts was determined. Voxels with

**TABLE 1.** Commonly Used Parameters from Dynamic Planar $^{99m}$Tc-GSA Scintigraphy

| Abbreviation | Parameter | Description | Mathematic formula | Application |
|---|---|---|---|---|
| LHL15 | Hepatic uptake ratio of $^{99m}$Tc-GSA | Liver counts at 15 min (L15) divided by heart counts (H15) plus L15 | $LHL\,15 = \frac{L15}{L15+H15}$ | Total liver function and regional liver function |
| HH15 | Blood clearance ratio | Heart counts at 15 min (H15) divided by heart counts at 3 min (H3) | $HH15 = \frac{H15}{H3}$ | Total liver function |
| MRI | Modified receptor index | LHL15 divided by HH15 | $MRI = \frac{LHL15}{HH15}$ | Total liver function |
| $K_L$ | Blood clearance constant | Calculated from liver uptake curve, with clearance half-time ($T_{1/2}$) (Fig.1) | $Liver\,uptake\,(t) = C_0\,(1-e^{K_L t})$<br>$K_L = \frac{Ln\,2}{T_{1/2}}$ | Total liver function |
| LU15 | Liver uptake | Cumulative liver uptake 15–16 min after injection from liver time–activity curve (L(t)) | $LU15 = \frac{\int_{15}^{16} L(t)dt}{total\,injected\,dose} \times 100$ | Total liver function |
| LHL15-V | Ratio of liver uptake to liver volume (mL) | Liver uptake ratio (LHL15) divided by total liver volume | $LHL15-V = \frac{LHL15}{preoperative\,liver\,volume} \times 1,000$ | Total liver function |
| $R_{max}$ | Maximal removal rate of $^{99m}$Tc-GSA | Calculated with kinetic model of Ha-Kawa et al. (*36*) | Requires multiple equations | Total liver function |
| $R_0$ | Asialoglycoprotein receptor concentration | Calculated with kinetic model of Vera et al. (*37*) | Requires multiple equations | Total liver function |

**TABLE 2.** Commonly Used Parameters Derived from $^{99m}$Tc-GSA SPECT

| Abbreviation | Parameter | Description | Mathematic formula | Application |
|---|---|---|---|---|
| FLV | Functional liver volume | Outline extraction method with specific cutoff level; sum of product of liver surface in each slice and slice thickness | $\sum(\text{liver surface} \times \text{slice thickness})$ | Total liver function; regional liver function |
| $K_u$ | Hepatic $^{99m}$Tc-GSA clearance | Patlak plot analysis: L(t) is liver activity, B(t) is blood activity, Vh is hepatic blood volume | $L(t)/B(t) = K_U \times \int_0^t B(\tau)d\tau/B(t)+Vh$ | Total liver function; regional liver function |
| LUR | Liver uptake ratio | Hepatic SPECT counts divided by injected syringe counts | $LUR = \frac{\text{total SPECT counts}}{\text{counts syringe preinjection}} \times 100$ | Total liver function; regional liver function |
| LUD | Liver uptake density | Liver uptake ratio divided by liver functional volume | $LUD = \frac{LUR}{\text{functional liver volume}}$ | Total liver function; regional liver function |
| PRI | Predictive residual index | Sum of product of blood clearance constant ($k_i$-value) and functional liver volume ($FLV_i$) in FRL in each slide divided by product of normal k-value (healthy volunteers) and total FLV | $PRI = \frac{\sum ki \times FLVi}{Kn \times FLV}$ | Regional liver function |
| FRR | Functional resection ratio | Counts in expected resection volume divided by counts in total liver volume | $FRR = \frac{\text{resection volume counts}}{\text{total liver volume counts}} \times 100$ | Regional liver function |

counts below 54% of the maximal counts were regarded as background. Voxels with counts above 80% of the maximum were considered fully functional, and their voxel thickness was counted as the maximal voxel thickness for the calculation of liver functional volume. For each voxel with counts between 54% and 80%, the voxel thickness was estimated according to the accumulated counts in that voxel.

In addition to static SPECT, dynamic SPECT has been applied. It requires a fast rotating multidetector γ-camera, which is not widely available. Liver uptake ratio and liver uptake density are calculated from dynamic SPECT acquisitions (*45,46*). Liver uptake ratio reflects the percentage of hepatic SPECT counts relative to the injected counts measured in the syringe, thereby calculating the dose that is incorporated in the liver. Liver uptake density is the liver uptake ratio divided by functional liver volume. In addition, the hepatic $^{99m}$Tc-GSA clearance ($K_u$, mL/min) can be calculated using a Patlak plot analysis (*42*).

## $^{99m}$Tc-GSA Liver Scintigraphy in Experimental Surgical Research

Small-animal models are commonly used to study the complex recovery mechanisms of liver function during liver regeneration. Recently, we studied the application of $^{99m}$Tc-GSA scintigraphy with SPECT for the assessment of liver function and functional volume during liver regeneration in a rat model (*47*). In normal rat livers, as well as in regenerating livers, a strong correlation was found between functional liver volume and conventional liver volume, indicating the usefulness of $^{99m}$Tc-GSA SPECT to measure functional liver volume in a noninvasive manner. The hepatic $^{99m}$Tc-GSA uptake measured by dynamic scintigraphy, however, seemed to underestimate hepatic regeneration in comparison to liver volume.

Unlike ICG, $^{99m}$Tc-GSA uptake is not directly inhibited by hyperbilirubinemia and can therefore be used to evaluate liver function during cholestasis. In a rat model of obstruc-

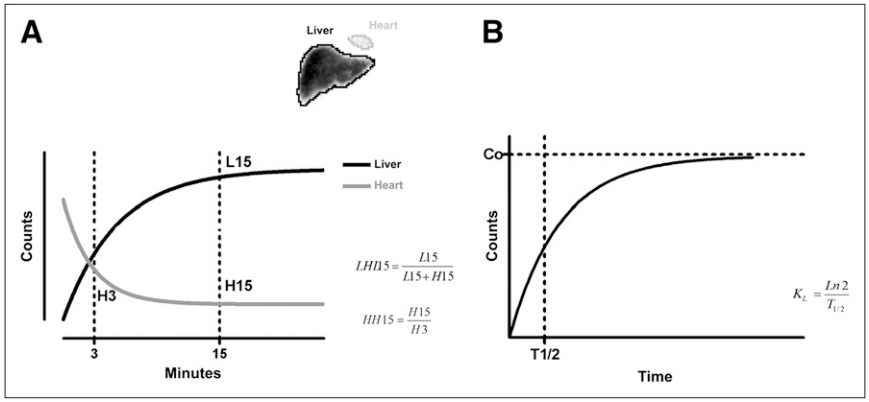


**FIGURE 1.** Planar dynamic $^{99m}$Tc-GSA scintigraphy. (A) LHL15 and HH15 are calculated from $^{99m}$Tc-GSA time–activity curves from heart (gray) and liver (black). (B) Blood clearance constant ($K_L$) is calculated from liver uptake curve using clearance half-time ($T_{1/2}$).

tive jaundice, hepatic $^{99m}$Tc-GSA uptake decreased as the period of jaundice was prolonged, as is explained by a decrease in affinity of the asialoglycoprotein receptor for $^{99m}$Tc-GSA (*34*).

## Clinical Use of $^{99m}$Tc-GSA Liver Scintigraphy in Liver Surgery

*Preoperative Assessment of Liver Function.* Multiple studies have described the application of preoperative planar dynamic $^{99m}$Tc-GSA scintigraphy for predicting postoperative complications (*31*,*48–50*). Preoperative GSA $R_{max}$ and LHL15 proved to be reliable indicators for predicting postoperative complications in patients with hepatocellular carcinoma and chronic liver disease, because significantly lower values were found in patients with major postoperative complications (*30,50*). Specific cutoff values for LHL15 (i.e., 0.90 (*48*) and 0.875 (*31*)) have been described to select patients with a high risk for complications. Other cutoff values include LHL15/preoperative liver volume of 0.76 (*32*) and total asialoglycoprotein receptor concentration in the FRL of 0.05 μmol (*31,49*). Cutoff values, however, usually are not based on accurate risk analysis but rather are set arbitrarily. In patients with a discrepancy between ICG15 and LHL15, $^{99m}$Tc-GSA scintigraphy was better in predicting postoperative complications (*31*). Multivariate analysis revealed that LHL15 was an independent preoperative predictor of postoperative complications in patients with chronic liver disease, whereas the ICG clearance test was not (*48*). Postoperative liver failure, however, was also observed in patients with relatively normal liver function (LHL15 > 0.875), as can be explained by the fact that LHL15 measures only preoperative total liver function and not FRL function.

Static $^{99m}$Tc-GSA SPECT was introduced for measurement of functional volume and more accurate assessment of segmental liver function (*33*,*42–44*). Whereas functional volume measured by $^{99m}$Tc-GSA SPECT reflects the functional hepatocyte mass (*43,51*), CT volumetry cannot distinguish between functional and nonfunctional liver tissue. This is especially of interest in cirrhotic patients, in whom advanced fibrosis is accompanied by a reduction of functional hepatocytes. In addition, tumor compression on surrounding liver tissue, bile ducts (*33*), or blood vessels (*52*) can affect regional liver function, whereas liver volume is maintained over a longer period. Preoperative functional volume measured by $^{99m}$Tc-GSA SPECT proved more suitable for predicting remnant liver function than did CT volumetry in a study group with predominantly cirrhotic patients (*33,44*). Although the outline extraction method is regularly used to calculate functional hepatic volume (*33,44,52–54*), that method is based on the assumption that liver function is uniformly distributed in the tissue included within the cutoff value. Especially in tumor-bearing and compromised livers, function is not distributed homogeneously. Therefore, functional volume does not necessarily correlate with intrinsic liver function measured by dynamic planar $^{99m}$Tc-GSA scintigraphy (*41,43*).

To overcome this problem, dynamic SPECT was introduced. A study by Sugahara et al. demonstrated the advantage of dynamic SPECT for assessment of regional liver function (*55*). Liver functional volume (by outline extraction method), liver uptake ratio, and liver uptake density were calculated in patients with different severities of parenchymal liver disease. Both liver uptake ratio and liver uptake density decreased with the severity of liver disease, whereas functional liver volume was significantly decreased only in patients classified as Child–Pugh C. The ratio of liver uptake (and liver uptake density) between the left liver lobe and right lobe changed with the progression of liver disease, confirming that liver function is not distributed homogeneously in patients with compromised livers. Dynamic SPECT was used to measure FRL function and preoperatively predict postoperative complications (*42,43*). Patients with postoperative liver insufficiency had significantly lower hepatic FRL $^{99m}$Tc-GSA clearance ($K_u$, in mL/min) than did patients without complications (*42*). The predictive residual index was able to predict postoperative complications with a positive predictive value of 71% and negative predictive value of 100%, using a cutoff value of 0.38 (*43*). The conclusions in these studies, however, were based on a relatively small number of complications.

*Increase of Liver Function After PVE.* Several studies evaluated increased FRL function after PVE using $^{99m}$Tc-GSA scintigraphy (*46,53–57*). In 2 studies, the increase in FRL function after PVE was measured by dynamic $^{99m}$Tc-GSA SPECT and was compared with an increase in FRL volume, measured by CT volumetry, in cirrhotic and noncirrhotic patients (*53,57*). The increase in FRL function (expressed as liver uptake ratio, liver uptake density, residual functional liver volume, and predictive residual index) was more extensive than the increase in FRL volume, indicating that $^{99m}$Tc-GSA scintigraphy has additional value over CT volumetry for evaluating the functional increase in FRL after PVE.

So far, no studies have been published on the use of $^{99m}$Tc-GSA scintigraphy in selecting candidates for PVE. Therefore, further research in this field is recommended.

*Postoperative Liver Regeneration.* Postoperative liver regeneration is currently evaluated by CT volumetry. A discrepancy has been described between postoperative liver functional recovery and volumetric liver regeneration. Tanaka et al. reported that functional recovery was impaired after large resections, in comparison to volumetric regeneration (*41*). However, data presented in this study demonstrated that 4 wk after a resection, the average LHL15 recovered to 95% of the preoperatively measured value, whereas volume recovered to approximately 70% of initial values. This finding suggests that functional recovery was greater then volumetric recovery, indicating the opposite of the conclusions drawn by the authors. Kwon et al. described in 2 almost identical studies that functional regeneration was more rapid than volumetric regeneration measured by CT volumetry (*44,54*). Functional and volumetric liver regener-

ation was delayed in patients with underlying liver disease. Although no direct comparison was made between $^{99m}$Tc-GSA SPECT and CT volumetry, it was concluded that functional recovery was more rapid in patients with injured livers. Again, in our view, the data presented in these studies do not support this conclusion. Although $^{99m}$Tc-GSA scintigraphy is useful to assess liver regeneration, it is difficult to draw conclusions on the difference between functional and volumetric regeneration from the present evidence.

$^{99m}$Tc-GSA scintigraphy has also been used to preoperatively predict the rate of liver regeneration after partial hepatectomy in patients with liver fibrosis (*58*). $^{99m}$Tc-GSA scintigraphy correlates with the severity of liver fibrosis, and impaired liver regeneration is also described in patients with an increased severity of liver fibrosis (*59*). Patients with a high preoperative HH15 (>0.52) that was due to fibrosis exhibited a worse regeneration of the remnant liver (*58*).

### Clinical Use of $^{99m}$Tc-GSA Scintigraphy in Liver Transplantation

After liver transplantation, graft function is affected by many factors, including acute and chronic rejection, indicating the necessity to evaluate posttransplantation graft function. In a study comprising 7 liver transplant patients, the total amount of asialoglycoprotein receptors ($R_{tot}$ by the kinetic model of Miki et al. (*39,40*)) was used to evaluate liver allograft function (*60*). Histologic liver damage was evaluated from a biopsy sample and correlated with $R_{tot}$. Although cohort size was small, this study shows the potential of $^{99m}$Tc-GSA scintigraphy to noninvasively evaluate graft function after transplantation.

In an auxiliary partial orthotopic liver transplantation, the native liver is left partially in place and the donor (partial) liver graft is positioned orthotopically. $^{99m}$Tc-GSA scintigraphy can be used to monitor both graft and native liver function after auxiliary partial orthotopic liver transplantation (*61*). The uptake of $^{99m}$Tc-GSA (calculated by Patlak plot analysis) proved a better predictor of actual graft function than did liver volume assessed by CT volumetry. Especially in patients with severely damaged liver grafts, $^{99m}$Tc-GSA uptake corresponded better with histopathologic evaluation of liver biopsy than did CT volumetry.

In 2004, Kwon et al. addressed the need to accurately measure FRL function in donors participating in living donor liver transplantation (*62*). The authors concluded that the FRL function estimated by $^{99m}$Tc-GSA SPECT is useful for selecting the hepatectomy procedure in the setting of living donor liver transplantation. However, that study was performed on 152 patients resected predominantly for malignant tumors and not for living donor liver transplantation. Eighty-three percent of the patients were resected for hepatocellular carcinoma, which is frequently associated with liver cirrhosis. Therefore, it is highly questionable if the patients included in this study are representative of living donors.

## HBS WITH IDA DERIVATES

### Background

$^{99m}$Tc-IDA agents were introduced in 1976 by Loberg et al. (*63*). These lidocaine analogs are transported to the liver predominantly bound to albumin (*64*). Dissociation between albumin and the $^{99m}$Tc-IDA agents occurs in the hepatic space of Disse, after which the $^{99m}$Tc-IDA agents is taken up by the hepatocytes. Although IDA agents are not metabolized, they follow the path of intracellular transit similar to various endogenous and foreign substances, including bilirubin, hormones, drugs, and toxins, thus representing an important function of the liver (*64,65*). Organic anion transporter polypeptides, expressed in the basolateral plasma membrane of hepatocytes, are involved in the uptake of organic anions. Organic anion transporter polypeptides 1B1 and 1B3 are able to transport $^{99m}$Tc-mebrofenin, which is an IDA derivate (*66*). IDA agents are excreted in the bile canaliculi similarly to ICG without undergoing biotransformation during their transport through the hepatocyte and, therefore, are ideal tracers for the biliary tract (*63,67*). The suggested bile canalicular transporters include multidrug resistance protein 2 (*66,68*).

$^{99m}$Tc-labeled IDA agents were first used in cholescintigraphy for the diagnosis of various biliary diseases (*64,69*). More recently, the application of HBS has been proposed for assessment of liver function (*70*). Liver uptake of IDA agents can be affected by high plasma levels of bilirubin (*69*). Of all IDA analogs, $^{99m}$Tc-mebrofenin shows the highest hepatic uptake, minimal urinary excretion, and strong resistance to displacement by high plasma bilirubin concentrations (*69,71*). Therefore, $^{99m}$Tc-mebrofenin is considered the most suitable agent for hepatic and biliary diagnostic procedures. $^{99m}$Tc-mebrofenin uptake can be hindered by hypoalbuminemia, as albumin is the main plasma carrier of $^{99m}$Tc-mebrofenin (*69*). Hypoalbuminemia consequently decreases hepatic delivery of $^{99m}$Tc-mebrofenin and increases renal excretion. Conversely, hypoalbuminemia in liver disease is a sign of impaired liver function and therefore decreased mebrofenin uptake in patients with hypoalbuminemia still reflects liver function.

### The Kinetics and Quantitative Measurement of Liver Function

Measurement of hepatic uptake function by the clearance rate of iodide (an IDA analog) was first described by Ekman et al. (*72*). The hepatic uptake of $^{99m}$Tc-mebrofenin is calculated similarly to iodide (*73*). After intravenous injection of $^{99m}$Tc-mebrofenin, dynamic scintigraphy is performed with a γ-camera. The hepatic uptake of $^{99m}$Tc-mebrofenin is determined by drawing an ROI around the liver, the heart (serving as blood pool), and the total field of view (Fig. 2). Three different time–activity curves based on these ROIs are generated. With these 3 parameters, the hepatic $^{99m}$Tc-mebrofenin uptake rate (%/min) can be calculated. Radioactivity values acquired between 150 and 350 s after injection are used to ensure that the calculations

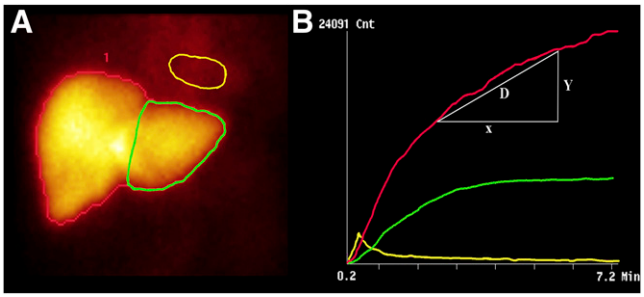


**FIGURE 2.** Dynamic image of planar HBS. (A) Example of summed HBS images from 150 to 350 s after intravenous injection of $^{99m}$Tc-mebrofenin. ROI is drawn around entire liver (red line), mediastinum (blood pool; yellow line), and FRL (green line). (B) Blood-pool–corrected liver uptake time–activity curve. Liver uptake of mebrofenin is calculated as increase of blood-pool–corrected $^{99m}$Tc-mebrofenin uptake (*y*-axis) per minute over a period of 200 s.

are made during a phase of homogeneous distribution of the agent in the blood pool, before biliary excretion takes place (*73,74*). To compensate for differences in individual metabolic requirements, hepatic $^{99m}$Tc-mebrofenin uptake rate (%/min) is divided by body surface area and expressed as %/min/m$^2$. ROIs can be drawn around specific parts of the liver to calculate regional differences in $^{99m}$Tc-mebrofenin uptake (Fig. 2). FRL uptake function is calculated by dividing counts within the ROI of the FRL by the total liver counts and multiplying this factor by total liver $^{99m}$Tc-mebrofenin uptake and is expressed as %/min/m$^2$. Regional uptake and FRL uptake of $^{99m}$Tc-mebrofenin can be assessed with little intra- and interobserver variation (*74,75*). Single-head γ-cameras permit anterior or posterior projections of the liver only. Dual-head γ-cameras enable simultaneous data acquisition of the anterior and posterior projections, from which a geometric mean dataset can be calculated, thereby reducing the attenuation bias (*76*).

Alternative methods for determining liver function include hepatic extraction fraction, the time at which maximal hepatic radioactivity occurs ($T_{peak}$), and the time required for peak activity to decrease by 50% ($T_{1/2\ peak}$) (*77–79*). The hepatic extraction fraction is calculated from the time–activity curves of the heart and liver by a deconvulsion analysis using a (modified) Fourier transform method (*80*).

Recently, application of $^{99m}$Tc-mebrofenin SPECT for the assessment of regional liver function and functional liver volume has been described (*76*). The timing of the SPECT is a challenge when a dynamic tracer is used, which is taken up by the liver and subsequently excreted in the bile. The SPECT acquisition is therefore centered on the peak of the hepatic time–activity curve, when the amount of radioactivity within the liver is relatively stable. In patients with fast hepatic uptake, biliary excretion is already visible during the SPECT phase, disturbing the calculation of total and regional liver function and volume. Activity within the extrahepatic bile ducts is therefore removed, and activity in the intrahepatic bile ducts is replaced by the average count density of normal liver tissue. Functional liver volume is calculated by the outline extraction method (with a threshold of 30% of the maximal voxel count value). The FRL can be outlined manually on a low-dose CT scan linked to the SPECT images, with a contrast-enhanced CT scan used as a reference. The percentage of counts within the FRL is calculated by dividing counts within the FRL by the total counts within the entire liver. For calculation of actual FRL function, this percentage is multiplied by the total liver $^{99m}$Tc-mebrofenin uptake rate as measured by the geometric mean dataset of the dynamic HBS.

## HBS in Experimental Surgical Research

Measurement of liver function in small animals remains a challenge because many quantitative liver function tests require repetitive blood samples. Hepatic extraction fraction and $T_{1/2\ peak}$, measured by HBS, were used as a noninvasive method of evaluating hepatic function after ischemia–reperfusion injury to quantify the protective effect of new interventions on ischemia–reperfusion injury (*81–83*).

For the evaluation of functional regeneration in small animals, serial measurements over a relatively long time period are preferred. The use of the hepatic $^{99m}$Tc-mebrofenin uptake rate measured by dedicated pinhole HBS has recently been validated in different rat models of liver regeneration (*77*). $^{99m}$Tc-mebrofenin HBS proved to be an accurate, noninvasive tool for the measurement of liver function in the rat and enabled serial measurements within the same animal (*77*).

## Clinical Use of HBS in Liver Surgery

*Preoperative Assessment of Liver Function.* The use of $^{99m}$Tc-mebrofenin HBS for preoperative assessment of liver function in patients undergoing liver surgery was first described by Erdogan et al. (*73*). In 54 patients scheduled for liver resection, $^{99m}$Tc-mebrofenin uptake measured by HBS strongly correlated with the ICG clearance test. Besides quantitative information, HBS provides visual information about the localization of liver segments with inferior function. Biliary excretion of $^{99m}$Tc-mebrofenin is useful for preoperatively determining segmental cholestasis and for diagnosing postoperative biliary complications, such as bile leakage and biliary obstructions. Because of the possibility of determining regional liver function, HBS was validated as a preoperative method for estimating FRL function (*74*). In this relatively small patient study, preoperatively estimated FRL function correlated well with actual remnant liver function 1 d after resection.

Dinant et al. investigated the value of preoperative FRL function, measured by $^{99m}$Tc-mebrofenin HBS, in predicting short-term outcome after partial liver resection (*75*). Forty-six patients with and without parenchymal disease were included in this study. Preoperative measurement of FRL function was more accurate than liver volume in predicting postoperative liver failure and liver failure–related mortality. A safe resection could be performed in patients with FRL uptake

above 2.5%/min/m$^2$ of body surface area, with a 3% chance of developing postoperative liver failure and liver failure–related mortality. However, in patients with FRL uptake below 2.5%/min/m$^2$, the risk of postoperative liver failure increased to 56%. In high-risk patients undergoing major liver resection, receiver-operating-characteristic curve analysis yielded a similar FRL function cutoff of 2.69%/min/m$^2$ (*84*). HBS takes into account the presence of underlying parenchymal liver disease, with compromised livers having significantly less liver function. Therefore, a single cutoff value for the prediction of liver failure suffices for both patients with a compromised liver and patients with a normal liver. In patients with an unknown quality of liver parenchyma, preoperative dynamic HBS proved more valuable then CT volumetry for the prediction of postoperative liver failure (*75*, *84*).

In the 2 abovementioned studies published by Erdogan and Dinant, HBS parameters have been derived from a single-head γ-camera using only the anterior projection (*75,84*). Because of the anatomic position of the liver, the left hemiliver is situated more anteriorly, leading to an overestimation of segmental left liver function in the anterior projection. The increasing availability of dual-head rotating γ-cameras enables the calculation of a geometric mean dataset of the anterior and posterior projections, which is recommended for dynamic HBS in the future.

Although dynamic $^{99m}$Tc-mebrofenin HBS has the possibility of measuring regional liver function, the 2-dimensional planar images lack the ability to assess detailed liver function on a segmental level. Modern SPECT/CT cameras combine dynamic $^{99m}$Tc-mebrofenin HBS with additional SPECT and the anatomic information of the CT scan, thereby enabling measurement of segmental liver function and functional liver volume. A recent study including 36 patients demonstrated that $^{99m}$Tc-mebrofenin SPECT provided valuable visible information on the distribution of liver function (Fig. 3.) (*76*) The results of functional liver volume measured by SPECT and morphologic volume measured by CT volumetry indicated that SPECT was an accurate method of measuring hepatic volume. FRL function measured by the combination of SPECT and dynamic HBS was able to accurately predict the actual function of the postoperative remnant liver.

*Increase of Liver Function After PVE.* The application of $^{99m}$Tc-mebrofenin HBS after PVE is currently under investigation. HBS is one of the few quantitative liver function tests that has the ability to measure regional liver function and is therefore ideal for evaluating the functional increase in FRL after PVE. In addition, HBS could potentially be used to decide on candidates for PVE because of the ability to select patients with an increased risk of postoperative liver failure (*75*).

*Postoperative Liver Regeneration.* Bennink et al. compared the volumetric regeneration 3 mo after partial liver resection with the functional regeneration measured by HBS and ICG15 (*74*). There was a significant correlation between the ICG clearance and HBS. However, a weak association between functional recovery (HBS and ICG) and volumetric regeneration (CT volumetry) was observed. This discrepancy confirms that the mechanisms of functional recovery may be independent of those controlling volumetric regeneration.

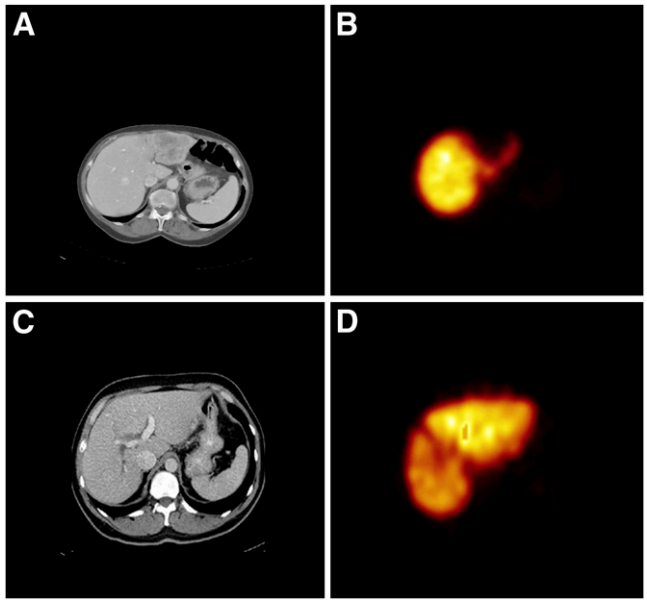


**FIGURE 3.** Two examples of $^{99m}$Tc-mebrofenin SPECT, with CT scans on left and matching SPECT images on right. (A and B) Patient with large colorectal metastasis in left liver segments, visible on CT scan. SPECT image shows inhomogeneous distribution of mebrofenin, with decreased uptake in liver segments 2–4. (C and D) Patient with colorectal metastasis (not visible on this CT slide) in which tumor is compressing surrounding vessels and bile ducts, resulting in impaired liver function in segments 5–8.

## Clinical Use of HBS in Liver Transplantation

Biliary complications and hepatic dysfunction due to graft rejection are major causes of postoperative morbidity and mortality in liver transplant recipients. Many studies have shown that HBS is an accurate, noninvasive technique for the diagnosis of biliary complications, including segmental and total biliary obstruction, as well as bile leakage in adult and pediatric transplantation patients (*85–88*). The efficacy of HBS for detection of graft dysfunction because of rejection is unclear. Graft rejection is usually diagnosed by liver biopsy. Brunot et al. demonstrated a close relation between early biopsy results and liver uptake function measured by HBS, implying that HBS is valuable in distinguishing graft rejection from cholestasis (*89*). In contrast, others reported that HBS can distinguish between normal grafts and those experiencing rejection or cholestasis but not between biliary complications and rejection (*85,90*).

In heterotopic auxiliary liver transplantation, the native liver is left in situ and a partial liver graft is transplanted elsewhere in the abdominal cavity. It has occasionally been

applied in patients with fulminant liver failure, in whom the native liver is expected to recover and regain function. Individual assessment of graft and native liver is difficult because most function tests measure total liver function. HBS has the unique ability to perform functional assessment of graft and native liver separately (*91,92*).

Because of an increased shortage of cadaveric liver grafts, living donor liver transplantation is used to expand the organ pool. In living donor liver transplantation, a left or right hepatectomy is performed on a living donor. The regeneration capacity in donors after living donor liver transplantation was investigated using HBS (*93*). As described by others, that study indicated that accelerated recovery of organ function is an early compensatory mechanism after reduction of organ volume (*93*). To date, no studies have been published using HBS for the preoperative assessment of liver function in the donor in living donor liver transplantation.

## DISCUSSION

$^{99m}$Tc-GSA scintigraphy and $^{99m}$Tc-mebrofenin HBS are simple techniques that can be implemented in every hospital with a nuclear medicine department. Both methods are applicable in patients with parenchymal liver disease, which is of increasing importance in view of the increasing number of patients presenting with parenchymal liver disease due to neoadjuvant chemotherapy or aspects of Western lifestyle such as obesity, alcohol consumption, and sexually transmitted diseases.

$^{99m}$Tc-GSA scintigraphy and $^{99m}$Tc-mebrofenin HBS are based on 2 different principles. $^{99m}$Tc-GSA scintigraphy measures the binding of $^{99m}$Tc-GSA to its receptor expressed on hepatocytes. A decreased hepatic $^{99m}$Tc-GSA uptake can be caused by a reduction in the $^{99m}$Tc-GSA binding affinity (as seen in cholestasis (*34*)), a reduction in the amount of asialoglycoprotein receptors per hepatocyte, or a decrease in the number of hepatocytes (as seen in cirrhosis (*94*)). Because $^{99m}$Tc-GSA is not excreted into the bile, $^{99m}$Tc-GSA scintigraphy cannot be used to diagnose biliary complications after liver surgery or transplantation. HBS measures the hepatic uptake and excretion of $^{99m}$Tc-mebrofenin and therefore has the ability to also visualize the biliary system. Uptake of $^{99m}$Tc-mebrofenin can be influenced by hepatic blood flow, hypoalbuminemia, and high concentrations of bilirubin (*69*). Because the hepatic uptake of many substances is influenced by the same factors, it still reflects liver function under these conditions.

Compared with other dynamic quantitative liver function tests such as the ICG clearance test, $^{99m}$Tc-GSA scintigraphy and $^{99m}$Tc-mebrofenin HBS have the advantage of being able to measure both total and regional liver function, enabling functional assessment of specifically the FRL. For this reason, preoperative $^{99m}$Tc-GSA scintigraphy and HBS are accurate methods for preoperative prediction of postoperative complications (*31,42,48,75,84*) and for follow-up of FRL function after PVE.

Although both nuclear imaging techniques are applicable for the assessment of liver function in small laboratory animals, $^{99m}$Tc-GSA SPECT is preferred for the noninvasive assessment of liver functional volume. Dynamic SPECT acquisitions with $^{99m}$Tc-mebrofenin are difficult using dedicated animal pinhole γ-cameras because of the longer acquisition time per frame and faster hepatic uptake of $^{99m}$Tc-mebrofenin in rats.

Although many studies have proven the value of nuclear imaging in liver surgery and transplantation, these techniques are not widely used. $^{99m}$Tc-GSA scintigraphy is mainly used in Japan, whereas its use is not approved in Europe and the United States. In addition, $^{99m}$Tc-GSA scintigraphy uses many different, sometimes complex, parameters (Tables 1 and 2), making comparison of studies difficult. The application of $^{99m}$Tc-mebrofenin HBS in liver surgery is relatively new, and only a few clinical trials have been performed. Clinical trials on larger patient populations are required to confirm the value of $^{99m}$Tc-mebrofenin HBS for the preoperative assessment of liver function and the postoperative evaluation of complications and liver regeneration.

## CONCLUSION

Both $^{99m}$Tc-GSA scintigraphy and $^{99m}$Tc-mebrofenin HBS are noninvasive, reliable techniques that provide visual and quantitative information on both total and regional liver function. Both tests are applicable in patients with normal livers and patients with compromised livers. These features render both $^{99m}$Tc-GSA scintigraphy and $^{99m}$Tc-mebrofenin HBS useful tests for the assessment of liver function in liver surgery and liver transplantation.

## REFERENCES


1. Shoup M, Gonen M, D'Angelica M, et al. Volumetric analysis predicts hepatic dysfunction in patients undergoing major liver resection. *J Gastrointest Surg.* 2003;7:325–330.
2. Shirabe K, Shimada M, Gion T, et al. Postoperative liver failure after major hepatic resection for hepatocellular carcinoma in the modern era with special reference to remnant liver volume. *J Am Coll Surg.* 1999;188:304–309.
3. Abdalla EK, Hicks ME, Vauthey JN. Portal vein embolization: rationale, technique and future prospects. *Br J Surg.* 2001;88:165–175.
4. Abulkhir A, Limongelli P, Healey AJ, et al. Preoperative portal vein embolization for major liver resection: a meta-analysis. *Ann Surg.* 2008;247:49–57.
5. Farges O, Belghiti J, Kianmanesh R, et al. Portal vein embolization before right hepatectomy: prospective clinical trial. *Ann Surg.* 2003;237:208–217.
6. Yamanaka N, Okamoto E, Kawamura E, et al. Dynamics of normal and injured human liver regeneration after hepatectomy as assessed on the basis of computed tomography and liver function. *Hepatology.* 1993;18:79–85.
7. Schneider PD. Preoperative assessment of liver function. *Surg Clin North Am.* 2004;84:355–373.
8. Nagashima I, Takada T, Okinaga K, Nagawa H. A scoring system for the assessment of the risk of mortality after partial hepatectomy in patients with chronic liver dysfunction. *J Hepatobiliary Pancreat Surg.* 2005;12:44–48.
9. Paumgartner G. The handling of indocyanine green by the liver. *Schweiz Med Wochenschr.* 1975;105(17, suppl):1–30.
10. Tygstrup N. Determination of the hepatic elimination capacity (Lm) of galactose by single injection. *Scand J Clin Lab Invest Suppl.* 1966;18:118–125.
11. Lau H, Man K, Fan ST, Yu WC, Lo CM, Wong J. Evaluation of preoperative hepatic function in patients with hepatocellular carcinoma undergoing hepatectomy. *Br J Surg.* 1997;84:1255–1259.

12. Yamanaka N, Okamoto E, Toyosaka A, et al. Prognostic factors after hepatectomy for hepatocellular carcinomas: a univariate and multivariate analysis. *Cancer.* 1990; 65:1104–1110.
13. Redaelli CA, Dufour JF, Wagner M, et al. Preoperative galactose elimination capacity predicts complications and survival after hepatic resection. *Ann Surg.* 2002;235:77–85.
14. Lam CM, Fan ST, Lo CM, Wong J. Major hepatectomy for hepatocellular carcinoma in patients with an unsatisfactory indocyanine green clearance test. *Br J Surg.* 1999;86:1012–1017.
15. Breitenstein S, Dimitroulis D, Petrowsky H, Puhan MA, Mullhaupt B, Clavien PA. Systematic review and meta-analysis of interferon after curative treatment of hepatocellular carcinoma in patients with viral hepatitis. *Br J Surg.* 2009;96: 975–981.
16. Ravaioli M, Grazi GL, Principe A, et al. Operative risk by the lidocaine test (MEGX) in resected patients for HCC on cirrhosis. *Hepatogastroenterology.* 2003;50:1552–1555.
17. Ercolani G, Grazi GL, Calliva R, et al. The lidocaine (MEGX) test as an index of hepatic function: its clinical usefulness in liver surgery. *Surgery.* 2000;127:464–471.
18. Vauthey JN, Chaoui A, Do KA, et al. Standardized measurement of the future liver remnant prior to extended liver resection: methodology and clinical associations. *Surgery.* 2000;127:512–519.
19. Clavien PA, Emond J, Vauthey JN, Belghiti J, Chari RS, Strasberg SM. Protection of the liver during hepatic surgery. *J Gastrointest Surg.* 2004;8:313–327.
20. Ratziu V, Charlotte F, Heurtier A, et al. Sampling variability of liver biopsy in nonalcoholic fatty liver disease. *Gastroenterology.* 2005;128:1898–1906.
21. Lindor KD, Bru C, Jorgensen RA, et al. The role of ultrasonography and automatic-needle biopsy in outpatient percutaneous liver biopsy. *Hepatology.* 1996;23:1079–1083.
22. McGill DB, Rakela J, Zinsmeister AR, Ott BJ. A 21-year experience with major hemorrhage after percutaneous liver biopsy. *Gastroenterology.* 1990;99:1396–1400.
23. Akaki S, Mitsumori A, Kanazawa S, et al. Technetium-99m-DTPA-galactosyl human serum albumin liver scintigraphy evaluation of regional CT/MRI attenuation/signal intensity differences. *J Nucl Med.* 1998;39:529–532.
24. Marshall JS, Green AM, Pensky J, Williams S, Zinn A, Carlson DM. Measurement of circulating desialylated glycoproteins and correlation with hepatocellular damage. *J Clin Invest.* 1974;54:555–562.
25. Sawamura T, Kawasato S, Shiozaki Y, Sameshima Y, Nakada H, Tashiro Y. Decrease of a hepatic binding protein specific for asialoglycoproteins with accumulation of serum asialoglycoproteins in galactosamine-treated rats. *Gastroenterology.* 1981;81:527–533.
26. Vera DR, Krohn KA, Stadalnik RC, Scheibe PO. Tc-99m-galactosyl-neoglycoalbumin: in vivo characterization of receptor-mediated binding to hepatocytes. *Radiology.* 1984;151:191–196.
27. Kokudo N, Vera DR, Makuuchi M. Clinical application of TcGSA. *Nucl Med Biol.* 2003;30:845–849.
28. Sasaki N, Shiomi S, Iwata Y, et al. Clinical usefulness of scintigraphy with $^{99m}$Tc-galactosyl-human serum albumin for prognosis of cirrhosis of the liver. *J Nucl Med.* 1999;40:1652–1656.
29. Kwon AH, Ha-Kawa SK, Uetsuji S, Kamiyama Y, Tanaka Y. Use of technetium 99m diethylenetriamine-pentaacetic acid-galactosyl-human serum albumin liver scintigraphy in the evaluation of preoperative and postoperative hepatic functional reserve for hepatectomy. *Surgery.* 1995;117:429–434.
30. Kwon AH, Ha-Kawa SK, Uetsuji S, Inoue T, Matsui Y, Kamiyama Y. Preoperative determination of the surgical procedure for hepatectomy using technetium-99m-galactosyl human serum albumin ($^{99m}$Tc-GSA) liver scintigraphy. *Hepatology.* 1997;25:426–429.
31. Nanashima A, Yamaguchi H, Shibasaki S, et al. Relationship between indocyanine green test and technetium-99m galactosyl serum albumin scintigraphy in patients scheduled for hepatectomy: clinical evaluation and patient outcome. *Hepatol Res.* 2004;28:184–190.
32. Fujioka H, Kawashita Y, Kamohara Y, et al. Utility of technetium-99m-labeled-galactosyl human serum albumin scintigraphy for estimating the hepatic functional reserve. *J Clin Gastroenterol.* 1999;28:329–333.
33. Mitsumori A, Nagaya I, Kimoto S, et al. Preoperative evaluation of hepatic functional reserve following hepatectomy by technetium-99m galactosyl human serum albumin liver scintigraphy and computed tomography. *Eur J Nucl Med.* 1998;25:1377–1382.
34. Mimura T, Hamazaki K, Sakai H, Tanaka N, Mimura H. Evaluation of hepatic functional reserve in rats with obstructive jaundice by asyaloglycoprotein receptor. *Hepatogastroenterology.* 2001;48:777–782.
35. Vera DR, Stadalnik RC, Trudeau WL, Scheibe PO, Krohn KA. Measurement of receptor concentration and forward-binding rate constant via radiopharmacokinetic modeling of technetium-99m-galactosyl-neoglycoalbumin. *J Nucl Med.* 1991;32:1169–1176.
36. Kudo M, Todo A, Ikekubo K, Yamamoto K, Vera DR, Stadalnik RC. Quantitative assessment of hepatocellular function through in vivo radioreceptor imaging with technetium 99m galactosyl human serum albumin. *Hepatology.* 1993;17:814–819.
37. Vera DR, Stadalnik RC, Metz CE, Pimstone NR. Diagnostic performance of a receptor-binding radiopharmacokinetic model. *J Nucl Med.* 1996;37:160–164.
38. Ha-Kawa SK, Tanaka Y. A quantitative model of technetium-99m-DTPA-galactosyl-HSA for the assessment of hepatic blood flow and hepatic binding receptor. *J Nucl Med.* 1991;32:2233–2240.
39. Miki K, Kubota K, Kokudo N, Inoue Y, Bandai Y, Makuuchi M. Asialoglycoprotein receptor and hepatic blood flow using technetium-99m-DTPA-galactosyl human serum albumin. *J Nucl Med.* 1997;38:1798–1807.
40. Miki K, Kubota K, Inoue Y, Vera DR, Makuuchi M. Receptor measurements via Tc-GSA kinetic modeling are proportional to functional hepatocellular mass. *J Nucl Med.* 2001;42:733–737.
41. Tanaka A, Shinohara H, Hatano E, et al. Perioperative changes in hepatic function as assessed by asialoglycoprotein receptor indices by technetium 99m galactosyl human serum albumin. *Hepatogastroenterology.* 1999;46:369–375.
42. Hwang EH, Taki J, Shuke N, et al. Preoperative assessment of residual hepatic functional reserve using $^{99m}$Tc-DTPA-galactosyl-human serum albumin dynamic SPECT. *J Nucl Med.* 1999;40:1644–1651.
43. Satoh K, Yamamoto Y, Nishiyama Y, Wakabayashi H, Ohkawa M. $^{99m}$Tc-GSA liver dynamic SPECT for the preoperative assessment of hepatectomy. *Ann Nucl Med.* 2003;17:61–67.
44. Kwon AH, Matsui Y, Ha-Kawa SK, Kamiyama Y. Functional hepatic volume measured by technetium-99m-galactosyl-human serum albumin liver scintigraphy: comparison between hepatocyte volume and liver volume by computed tomography. *Am J Gastroenterol.* 2001;96:541–546.
45. Onodera Y, Takahashi K, Togashi T, Sugai Y, Tamaki N, Miyasaka K. Clinical assessment of hepatic functional reserve using $^{99m}$Tc DTPA galactosyl human serum albumin SPECT to prognosticate chronic hepatic diseases: validation of the use of SPECT and a new indicator. *Ann Nucl Med.* 2003;17:181–188.
46. Sugai Y, Komatani A, Hosoya T, Yamaguchi K. Response to percutaneous transhepatic portal embolization: new proposed parameters by $^{99m}$Tc-GSA SPECT and their usefulness in prognostic estimation after hepatectomy. *J Nucl Med.* 2000; 41:421–425.
47. de Graaf W, Vetelainen RL, de Bruin K, van Vliet AK, van Gulik TM, Bennink RJ. $^{99m}$Tc-GSA scintigraphy with SPECT for assessment of hepatic function and functional volume during liver regeneration in a rat model of partial hepatectomy. *J Nucl Med.* 2008;49:122–128.
48. Kim YK, Nakano H, Yamaguchi M, et al. Prediction of postoperative decompensated liver function by technetium-99m galactosyl-human serum albumin liver scintigraphy in patients with hepatocellular carcinoma complicating chronic liver disease. *Br J Surg.* 1997;84:793–796.
49. Kokudo N, Vera DR, Tada K, et al. Predictors of successful hepatic resection: prognostic usefulness of hepatic asialoglycoprotein receptor analysis. *World J Surg.* 2002;26:1342–1347.
50. Takeuchi S, Nakano H, Kim YK, et al. Predicting survival and post-operative complications with Tc-GSA liver scintigraphy in hepatocellular carcinoma. *Hepatogastroenterology.* 1999;46:1855–1861.
51. Wu J, Ishikawa N, Takeda T, et al. The functional hepatic volume assessed by $^{99m}$Tc-GSA hepatic scintigraphy. *Ann Nucl Med.* 1995;9:229–235.
52. Akaki S, Okumura Y, Sasai N, et al. Hepatectomy simulation discrepancy between radionuclide receptor imaging and CT volumetry: influence of decreased unilateral portal venous flow. *Ann Nucl Med.* 2003;17:23–29.
53. Hirai I, Kimura W, Fuse A, Suto K, Urayama M. Evaluation of preoperative portal embolization for safe hepatectomy, with special reference to assessment of nonembolized lobe function with $^{99m}$Tc-GSA SPECT scintigraphy. *Surgery.* 2003;133:495–506.
54. Kwon AH, Matsui Y, Kaibori M, Kamiyama Y. Functional hepatic regeneration following hepatectomy using galactosyl-human serum albumin liver scintigraphy. *Transplant Proc.* 2004;36:2257–2260.
55. Sugahara K, Togashi H, Takahashi K, et al. Separate analysis of asialoglycoprotein receptors in the right and left hepatic lobes using Tc-GSA SPECT. *Hepatology.* 2003;38:1401–1409.
56. Kubo S, Shiomi S, Tanaka H, et al. Evaluation of the effect of portal vein embolization on liver function by $^{99m}$Tc-galactosyl human serum albumin scintigraphy. *J Surg Res.* 2002;107:113–118.
57. Nishiyama Y, Yamamoto Y, Hino I, Satoh K, Wakabayashi H, Ohkawa M. $^{99m}$Tc galactosyl human serum albumin liver dynamic SPET for pre-operative assessment of hepatectomy in relation to percutaneous transhepatic portal embolization. *Nucl Med Commun.* 2003;24:809–817.

58. Iguchi T, Sato S, Kouno Y, et al. Comparison of Tc-99m-GSA scintigraphy with hepatic fibrosis and regeneration in patients with hepatectomy. *Ann Nucl Med.* 2003;17:227–233.
59. Koniaris LG, McKillop IH, Schwartz SI, Zimmers TA. Liver regeneration. *J Am Coll Surg.* 2003;197:634–659.
60. Kita Y, Miki K, Hirao S, et al. Liver allograft functional reserve estimated by total asialoglycoprotein receptor amount using Tc-GSA liver scintigraphy. *Transplant Proc.* 1998;30:3277–3278.
61. Sakahara H, Kiuchi T, Nishizawa S, et al. Asialoglycoprotein receptor scintigraphy in evaluation of auxiliary partial orthotopic liver transplantation. *J Nucl Med.* 1999;40:1463–1467.
62. Kwon AH, Matsui Y, Kaibori M, Satoi S, Kamiyama Y. Safety of hepatectomy for living donors as evaluated using asialoscintigraphy. *Transplant Proc.* 2004; 36:2239–2242.
63. Loberg MD, Cooper M, Harvey E, Callery P, Faith W. Development of new radiopharmaceuticals based on N-substitution of iminodiacetic acid. *J Nucl Med.* 1976;17:633–638.
64. Krishnamurthy S, Krishnamurthy GT. Technetium-99m-iminodiacetic acid organic anions: review of biokinetics and clinical application in hepatology. *Hepatology.* 1989;9:139–153.
65. Krishnamurthy GT, Krishnamurthy S. Cholescintigraphic measurement of liver function: how is it different from other methods? *Eur J Nucl Med Mol Imaging.* 2006;33:1103–1106.
66. Ghibellini G, Leslie EM, Pollack GM, Brouwer KL. Use of Tc-99m mebrofenin as a clinical probe to assess altered hepatobiliary transport: integration of in vitro, pharmacokinetic modeling, and simulation studies. *Pharm Res.* 2008;25: 1851–1860.
67. Trauner M, Meier PJ, Boyer JL. Molecular pathogenesis of cholestasis. *N Engl J Med.* 1998;339:1217–1227.
68. Hendrikse NH, Kuipers F, Meijer C, et al. In vivo imaging of hepatobiliary transport function mediated by multidrug resistance associated protein and P-glycoprotein. *Cancer Chemother Pharmacol.* 2004;54:131–138.
69. Krishnamurthy GT, Krishnamurthy S. *Nuclear Hepatology: A Textbook of Hepatobiliary Diseases.* New York, NY: Springer; 2000:38–51.
70. Heyman S. Hepatobiliary scintigraphy as a liver function test. *J Nucl Med.* 1994; 35:436–437.
71. Lan JA, Chervu LR, Johansen KL, Wolkoff AW. Uptake of technetium 99m hepatobiliary imaging agents by cultured rat hepatocytes. *Gastroenterology.* 1988;95:1625–1631.
72. Ekman M, Fjalling M, Holmberg S, Person H. IODIDA clearance rate: a method for measuring hepatocyte uptake function. *Transplant Proc.* 1992; 24:387–388.
73. Erdogan D, Heijnen BH, Bennink RJ, et al. Preoperative assessment of liver function: a comparison of $^{99m}$Tc-mebrofenin scintigraphy with indocyanine green clearance test. *Liver Int.* 2004;24:117–123.
74. Bennink RJ, Dinant S, Erdogan D, et al. Preoperative assessment of postoperative remnant liver function using hepatobiliary scintigraphy. *J Nucl Med.* 2004;45:965–971.
75. Dinant S, de Graaf W, Verwer BJ, et al. Risk assessment of posthepatectomy liver failure using hepatobiliary scintigraphy and CT volumetry. *J Nucl Med.* 2007;48:685–692.
76. de Graaf W, van Lienden KP, van Gulik TM, Bennink RJ. $^{99m}$Tc-mebrofenin hepatobiliary scintigraphy with SPECT for the assessment of hepatic function and liver functional volume before partial hepatectomy. *J Nucl Med.* 2010;51: 229–236.
77. Bennink RJ, Vetelainen R. de BK, van Vliet AK, van Gulik TM. Imaging of liver function with dedicated animal dynamic pinhole scintigraphy in rats. *Nucl Med Commun.* 2005;26:1005–1012.
78. Karamanlioglu B, Yuksel M, Temiz E, Salihoglu YS, Ciftci S. Hepatobiliary scintigraphy for evaluating the hepatotoxic effect of halothane and the protective effect of catechin in comparison with histo-chemical analysis of liver tissue. *Nucl Med Commun.* 2002;23:53–59.
79. Malhi H, Bhargava KK, Afriyie MO, et al. $^{99m}$Tc-mebrofenin scintigraphy for evaluating liver disease in a rat model of Wilson's disease. *J Nucl Med.* 2002;43: 246–252.
80. Brown PH, Juni JE, Lieberman DA, Krishnamurthy GT. Hepatocyte versus biliary disease: a distinction by deconvolutional analysis of technetium-99m IDA time-activity curves. *J Nucl Med.* 1988;29:623–630.
81. Chavez-Cartaya R, Ramirez P, Fuente T, et al. Blood clearance of $^{99m}$Tc-trimethyl-Br-IDA discriminates between different degrees of severe liver ischaemia–reperfusion injury in the rat. *Eur Surg Res.* 1997;29:346–355.
82. Yuksel M, Hatipoglu A, Temiz E, Salihoglu YS, Huseyinova G, Berkarda S. The role of hepatobiliary scintigraphy in the evaluation of the protective effects of dimethylsulphoxide in ischaemic/reperfusion injury of liver. *Nucl Med Commun.* 2000;21:775–780.
83. Veteläinen RL, Bennink RJ, de Bruin K, van Vliet A, van Gulik TM. Hepatobiliary function assessed by $^{99m}$Tc-mebrofenin cholescintigraphy in the evaluation of severity of steatosis in a rat model. *Eur J Nucl Med Mol Imaging.* 2006;33:1107–1114.
84. de Graaf W, van Lienden KP, Dinant S, et al. Assessment of future remnant liver function using hepatobiliary scintigraphy in patients undergoing major liver resection. *J Gastrointest Surg.* 2010;14:369–378.
85. Kim JS, Moon DH, Lee SG, et al. The usefulness of hepatobiliary scintigraphy in the diagnosis of complications after adult-to-adult living donor liver transplantation. *Eur J Nucl Med Mol Imaging.* 2002;29:473–479.
86. Kurzawinski TR, Selves L, Farouk M, et al. Prospective study of hepatobiliary scintigraphy and endoscopic cholangiography for the detection of early biliary complications after orthotopic liver transplantation. *Br J Surg.* 1997;84:620–623.
87. Mochizuki T, Tauxe WN, Dobkin J, et al. Detection of complications after liver transplantation by technetium-99m mebrofenin hepatobiliary scintigraphy. *Ann Nucl Med.* 1991;5:103–107.
88. Gelfand MJ, Smith HS, Ryckman FC, et al. Hepatobiliary scintigraphy in pediatric liver transplant recipients. *Clin Nucl Med.* 1992;17:542–549.
89. Brunot B, Petras S, Germain P, Vinee P, Constantinesco A. Biopsy and quantitative hepatobiliary scintigraphy in the evaluation of liver transplantation. *J Nucl Med.* 1994;35:1321–1327.
90. Engeler CM, Kuni CC, Nakhleh R, Engeler CE, duCret RP, Boudreau RJ. Liver transplant rejection and cholestasis: comparison of technetium 99m-diisopropyl iminodiacetic acid hepatobiliary imaging with liver biopsy. *Eur J Nucl Med.* 1992;19:865–870.
91. Buyck D, Bonnin F, Bernuau J, Belghiti J, Bok B. Auxiliary liver transplantation in patients with fulminant hepatic failure: hepatobiliary scintigraphic follow-up. *Eur J Nucl Med.* 1997;24:138–142.
92. Gencoglu E, Karakayali H, Moray G, Aktas A, Haberal M. Evaluation of pediatric liver transplant recipients using quantitative hepatobiliary scintigraphy. *Transplant Proc.* 2002;34:2160–2162.
93. Aktas A, Koyuncu A, Yalcin H. Acceleration of hepatobiliary dynamics in liver transplant donors. *Transplant Proc.* 2004;36:206–209.
94. Kawasaki S, Imamura H, Bandai Y, Sanjo K, Idezuki Y. Direct evidence for the intact hepatocyte theory in patients with liver cirrhosis. *Gastroenterology.* 1992; 102:1351–1355.

JNM The Journal of NUCLEAR MEDICINE

# Nuclear Imaging Techniques for the Assessment of Hepatic Function in Liver Surgery and Transplantation

Wilmar de Graaf, Roelof J. Bennink, Reeta Veteläinen and Thomas M. van Gulik

*J Nucl Med.* 2010;51:742-752.
Published online: April 15, 2010.
Doi: 10.2967/jnumed.109.069435



*The Journal of Nuclear Medicine* is published monthly.
SNMMI | Society of Nuclear Medicine and Molecular Imaging
1850 Samuel Morse Drive, Reston, VA 20190.
(Print ISSN: 0161-5505, Online ISSN: 2159-662X)



SNMMI SOCIETY OF NUCLEAR MEDICINE AND MOLECULAR IMAGING